Short Papers

Stable Broadband Microwave Amplifier Design Using the Simplified Real Frequency Technique

Wen-Lin Jung and Jung-Hui Chiu

Abstract—**Yarman's simplified real frequency technique is modified to design a stability-guaranteed broadband microwave amplifier consisting of a potentially unstable transistor. The source and load terminations can be complex impedances. The stability is maintained by the conductances resulted from transforming the source and load terminations through the input and output matching circuits. The input and output matching circuits are derived concurrently, instead of sequentially. Repeating the design of an example from a previous paper shows that the transducer gain obtained by using this method is higher, with fewer matching circuit elements, than that by using Supercompact optimizers. And, with the same number of matching circuit elements, the transducer gain is slightly higher than that by using the dynamic CAD technique.**

I. Introduction

The simplified real frequency technique of broadband matching has been applied to designing broadband amplifies [1], [2], [6]. This so-named technique is convenient in application because firstly, it utilizes (real frequency) directly measured impedance data, rather than rational functions or lumped circuit models, of the source and load circuits to design the matching circuit. Secondly, the shape of transducer gain is flexible, unrequired to be pre-assigned, such as Butterworth or Tchebyshev form. Thirdly, the matching circuit topology is derived by the method rather than pre-determined.

Since many microwave transistors are potentially unstable in the frequency band of interest, it is important that the stability be considered in broadband amplifier design. To the authors' knowledge, previous broadband amplifier design methods based on the simplified real frequency technique [1], [2], [6] have not taken the stability into account in the design procedure. One broadband stabilization idea is shunting a resistor to the output-port of the transistor to make it unconditionally stable [3]. But since the resistor dissipates signal power, the power gain will be decreased. In a recent paper [4], both the gain-flatness and stability are satisfied, by concurrently designing the input (front-end) and output (back-end) matching circuits to act not only as gain equalizers, but also as resistance transformers which transform the source and load terminating resistances to proper values needed for stabilization. However, to use this method, the source and load terminations must be pure resistances, not complex impedances. In addition, the matching circuits are designed by using the real frequency line-segment technique [5] which needs two approximations in realizing each matching circuit: the line-segment resistance approximation with resistive excursions as variables in the optimization stage, and then the construction of a physically realizable input impedance function by curve-fitting in the circuit synthesis stage.

In this paper, Yarman's simplified real frequency technique [1] is modified to design a broadband microwave amplifier with guaranteed stability. In the method to be proposed, the source and load terminations may be complex impedances. The input and output matching circuits are derived concurrently as in [4], not sequentially. The IMSL exact-gradient optimizer, DNCONG [7], are used for the gain optimization subject to stability constraints.

Manuscript received December 16, 1991; revised May 7, 1992. This work was supported by the National Science Council, Republic of China.

The authors are with the Department of Electronic Engineering, National Taiwan Institute of Technology, Taipei, Taiwan, 10772, Republic of China.

IEEE Log Number 9204490.

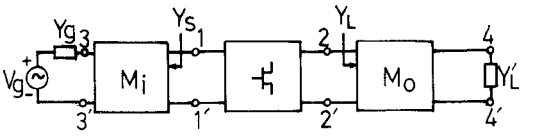

Fig. 1. Block diagram of an amplifier with complex source and load terminations.

Two examples are presented. In the first example, the proposed method is applied to design an 8–12 GHz amplifier with complex terminations. In the second example, two 6–18 GHz amplifiers with specifications taken from the literature [6] are designed using the proposed method. The first one has a higher gain, similar ripple, and fewer matching circuit elements, compared with that designed by Yarman using Supercompact [6]. The second one has a slightly higher gain, similar ripple and the same topology as Fig. 3 in reference [6] designed by the dynamic CAD technique. Although the transistors employed in both examples are potentially unstable, the amplifiers obtained are stable with specifiable minimum stability factor.

II. Principle

A. Stability and Transducer Power Gain

Let the y parameters of the transistor in Fig. 1 be denoted by

$$y_{ik} = g_{ik} + jb_{ik}, \qquad i,k = 1,2. \tag{1}$$

Assume, in Fig. 1, both the source and the load terminations, Y_g and Y_L', are complex admittances with positive real parts, and let the admittances looking into the lossless matching circuits M_i and M_o, respectively, from the transistor be

$$Y_s = G_s + jB_s, \qquad Y_L = G_L + jB_L \tag{2}$$

By Llewellyn's two-port stability criteria [10], the amplifier is unconditionally stable if, for all frequency, the inequalities in (3) hold

$$\begin{aligned} &G_s + g_{11} > 0, \qquad G_L + g_{22} > 0, \\ &(G_s + g_{11})(G_L + g_{22}) > \frac{M}{2}(1 + \cos\theta) \end{aligned} \tag{3}$$

where $M = |y_{12}\, y_{21}|$ and $\theta =$ phase of $(y_{12}\, y_{21})$. Based on the third inequality in (3), a stability factor, K, can be defined to indicate how stable an amplifier is [10],

$$K = \frac{[G_s + g_{11}][G_L + g_{22}]}{\frac{M}{2}[1 + \cos\theta]}. \tag{4}$$

Setting $G_s = G_L = 0$, (4) shows the intrinsic stability of a transistor. In terms of Y_s, Y_L and the y parameters of the transistor, the transducer power gain of the amplifier in Fig. 1 is given by [10]

$$G_T = \frac{4|y_{21}|^2 G_s G_L}{|(y_{11} + Y_s)(y_{22} + Y_L) - y_{12}y_{21}|^2}. \tag{5}$$

For convenience, in Fig. 1, the admittances Y_g, Y_L', Y_s, Y_L, and the transistor y parameters will be assumed to be normalized to 0.02 Siemens.

B. Lossless Matching Circuit Properties

Let the s-domain entries of the unit-normalized scattering matrix of M_i be $e_{ij}(s)$ and those for M_o be $f_{ij}(s)$, with $i, j = 1, 2$. The $e_{11}(s)$ and $f_{11}(s)$ will be referred to as input reflection function of M_i and M_o, respectively. Defining the ports connecting to the transistor as port-1 for both M_i and M_o, then it can be shown that

$$Y_s = \frac{1 - e_{11} - (e_{22} - \Delta_e)\gamma_g}{1 + e_{11} - (e_{22} + \Delta_e)\gamma_g},$$
$$Y_L = \frac{1 - f_{11} - (f_{22} - \Delta_f)\gamma_L'}{1 + f_{11} - (f_{22} + \Delta_f)\gamma_L'}, \tag{6}$$

where

$$\gamma_g = \frac{1 - Y_g}{1 + Y_g},$$
$$\Delta_e = e_{11}e_{22} - e_{12}e_{21},$$
$$\gamma_L' = \frac{1 - Y_L'}{1 + Y_L'},$$

and

$$\Delta_f = f_{11}f_{22} - f_{12}f_{21}.$$

Note that $e_{12} = e_{21}$ and $f_{12} = f_{21}$, for M_i and M_o are reciprocal. Assuming further that both M_i and M_o are ladders with all transmission zeros at infinity, then [1]

$$e_{11}(s) = \frac{h_e(s)}{g_e(s)},$$
$$e_{12}(s) = \frac{\pm s^k}{g_e(s)},$$
$$e_{22}(s) = -(-1)^k \frac{h_e(s)}{g_e(s)} \tag{7}$$

where $h_e(s) = h_{e0} + h_{e1}s + \cdots + h_{en}s^n$ is a polynomial with real coefficients, and $g_e(s) = g_{e0} + g_{e1}s + \cdots + g_{en}s^n$ is a strictly Hurwitz polynomial related to $h_e(s)$ in a lossless ladder as follows [1], [14]

$$g_e(s)\,g_e(-s) = h_e(s)\,h_e(-s) + (-1)^k s^{2k}. \tag{8}$$

The non-negative integer k in (7)–(8) determines the number of high-pass elements in ladder M_i. The integer n is the degree of both $h_e(s)$ and $g_e(s)$, and determines the number of elements in M_i.

A set of equations analogous to (7)–(8) can be set up for the lossless ladder M_o whose corresponding defining polynomials are $h_f(s)$ and $g_f(s)$. Certainly, the topology and complexity of ladder M_o can be different from that of M_i.

C. Design Theory

Let $G_T(i)$ and $G_o(i)$ be, respectively, the actual and the desired reference transducer gain at a sample frequency $\omega_i, i = 1, 2, \cdots, m$. Then a stable broadband amplifier, shown in Fig. 1, requires that the M_i and M_o be designed such that the objective function E defined below is minimized,

$$E = \sum_{i=1}^{m} \left[w(i) \left(\frac{G_T(i)}{\alpha G_o(i)} - 1 \right) \right]^2, \qquad G_o(i) > 0, \tag{9}$$

subject to the stability constraint defined at ω_i,

$$\frac{[G_s(i) + g_{11}(i)][G_L(i) + g_{22}(i)]}{\frac{M(i)}{2}[1 + \cos\theta(i)]} - K_{\min}(i) \geq 0,$$
$$i = 1, 2, \cdots, m \tag{10}$$

where $w(i)$ is the weighting factor at the ith sample frequency. The α is a constant, $0 < \alpha \leq 1$, used to modify the reference gain. The $K_{\min}(i)$ is referred to as the stability margin, should be unity for stability, and should be large enough to reduce interactions between the input and output matching circuits when $s_{12} \neq 0$ (bilateral transistors). It has been suggested that $K_{\min}(i) = 2$ [10]. The first and second inequalities in (3) can be ignored for many transistors whose g_{11} and g_{22} are positive for all frequencies in the band of potential unstability, and both G_s and G_L are non-negative for passive matching circuits and source and load terminations.

No realizability constraint needs to be considered since the strict Hurwitzness of $g_c(s)$ and $g_f(s)$ guarantees that both M_i and M_o are realizable.

Equation (10) shows that when $M \neq 0$ and $\theta \neq 180°$, the stability depends on the two coupled unknown functions G_s and G_L. Hence it is more convenient in broadband design to optimize the input and output matching circuits concurrently than to do sequentially.

For calculating the objective and constraint functions, first, the ladder type, k, and order n, are selected independently for M_i and M_o. Then, initial coefficients of $h_e(s)$ and $h_f(s)$ are selected. The polynomial $g_e(s)$ can be determined using (8) and its strict Hurwitzness property [14]. Knowing $h_e(s)$ and $g_e(s)$, the scattering matrix of M_i is established by (7). The scattering matrix of M_o can be established analogously. By (6), the $Y_s(i)$ and $Y_L(i)$ at any ω_i can be calculated. Using $Y_s(i), Y_L(i)$, and (5), the transducer gain $G_T(i)$ can be calculated. Finally, the objective function E is determined by (9) and the constraints by (10).

It has been found that the IMSL (in PC, Microsoft version) exact-gradient optimizer, DNCONG [7], based on quasi-Newton stepping and sequential quadratic programming, is suitable for the computation. The exact gradient of the objective function and that of the constraint functions can be derived using (8) and the implicit function theorem [15].

Since the input and output matching circuits are to be optimized simultaneously, the dimension of the unknown variables is higher in general, and so the selection of initial values (coefficients h_{ej} and h_{fj}) is more difficult than it is in the sequential design approach. The burden can be alleviated by starting design from order-1 matching circuits. Since now only two unknowns (h_{e1} and h_{f1}, if low-pass ladders are employed) are involved, error surfaces and constraints can be plotted to help the selection. However, experience in using the DNCONG reveals that the ad hoc initial values, ± 1 for h_{ej} and h_{fj}, suggested in the literature [1], [6] can also be directly employed for lower order matching circuits. Once a convergence is obtained by such trial runs, the resultant h_{ej} and h_{fj} can be used for improvement using the method proposed below.

The effective reference transducer gain at ω_i, $\alpha G_o(i)$, should not exceed the maximum transducer gain obtained by setting $y_{12}(i) = 0$ [10]. A reasonable value for α can be obtained after a few trial runs. Once a convergence is obtained, the possibility of higher G_T may be examined by re-executing the program using a slightly higher α and using the coefficients h_{ej} and h_{fj} just obtained as new initial values. Repeating this, the G_T can be gradually increased until the ripple becomes excessive. Note that each re-run, with a slightly increased α, starting from a point which is just obtained from the last run takes much less time than an initial trial run, because a new point associated with a slightly higher gain should not be far away from the point just found.

The possibility of using higher order M_i and/or M_o can be examined by using the results obtained from a lower order design. For instance, let $[0, h_{e1}, h_{e2}]$ be the three coefficients of $h_e(s)$, for an order-2 low-pass type M_i, obtained from a successful trial run using the ad hoc initial coefficients, then the possibility of using an order-3

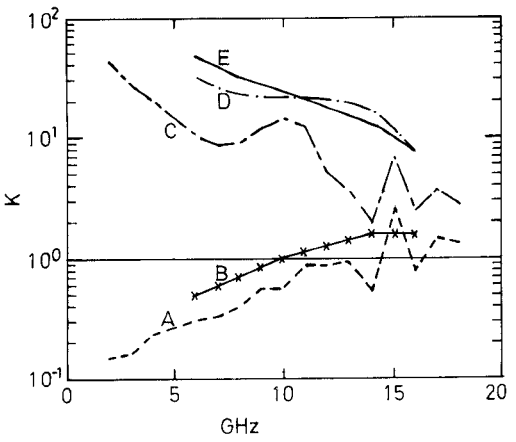

Fig. 2. Stability factors of transistors and amplifiers. Curve A: NE700, Curve B: HFET-2001. Curve C: amplifier in Fig. 3, Curve D: amplifier in Fig. 5, Curve E: amplifier in Fig. 4.

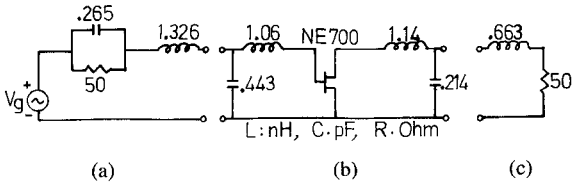

Fig. 3. Small signal schematic diagram of the amplifier in example 1. (a): source termination, (b): amplifier circuit, (c): load termination.

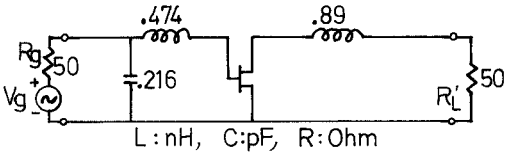

Fig. 4. Small signal schematic diagram of the amplifier in example 2, designed with $N_e = N_f = 2$. (A small capacitor of 18 μpF shunting R_L' has been neglected.)

low-pass type M_i can be examined by using $[0, h_{e1}, h_{e2}, \epsilon]$ as the initial coefficients of $h_e(s)$, where ϵ is a small quantity.

III. Examples

Example 1

This example demonstrates the use of the proposed method to design an 8–12 GHz amplifier with guaranteed stability. The source and load terminations are complex, shown in Fig. 3(a) and Fig. 3(c), respectively, taken from example 1 of [1] but frequency and impedance scaled to 12 GHz and 50 ohm. The transistor employed is an NEC MESFET, NE700, with $V_{ds} = 3$ V, and $I_{ds} = 30$ mA [11]. The y parameters at this operating point have been calculated and listed in [12]. The intrinsic stability factor K of NE700, as depicted by curve A in Fig. 2, shows that this transistor is potentially unstable in the range: 2–14 GHz.

A program, GTDRV, has been established for carrying out the computation. The program includes

1) a main section that reads, from an input data file, the lower and upper limits of coefficients h_{ej} and h_{fj}, the number of sample frequencies m, selected sample frequencies ω_i, transistor y parameters $y_{ik}(i)$, reflection coefficients of source and load terminations $\gamma_g(i)$ and $\gamma_L'(i)$, reference gains $G_o(i)$, and error weights $w(i)$. The main section then requests for the gain modifier α, degrees N_e of $h_e(s)$ and N_f of $h_f(s)$, initial guesses h_{ej} and h_{fj}, from the keyboard upon the GTDRV starting. After taking up all these data, the main section calls the IMSL subroutine DNCONG which interacts with the subroutines TRANSG and GRAD described below. Upon convergence, the subroutine OUTP described below is called to store the results to an output data file.
2) a subroutine, TRANSG, which calculates the objective function (9) and constraint functions (10). In addition to the built-in stopping criteria in the IMSL subroutine DNCONG, an exit is established in TRANSG to save execution time whenever possible. So the GTDRV will also stop whenever the relative gain error, $|G_T(i)/\alpha G_o(i) - 1|$, becomes sufficiently small and all the constraints are satisfied.
3) a subroutine, GRAD, which calculates the exact gradients of objective and constraint functions.
4) an outputting subroutine OUTP that stores, in an output data file, the input conditions: α, N_e, N_f, initial guesses h_{ej} and h_{fj}, and the optimized results: h_{ej}, g_{ej} for M_i, h_{fj} and g_{fj} for M_o, values of relative gain error, transducer gain, and constraint at each sample frequency.

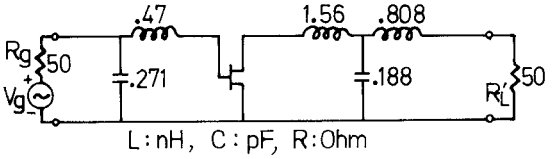

Fig. 5. Small signal schematic diagram of the amplifier in example 2, designed with $N_e = 2, N_f = 3$.

For this example:

The lower and upper limits of both h_{ej} and h_{fj} are set to be, -5 and 5, respectively.

$errlb = 0.15$, where $errlb \equiv$ range of acceptable $|G_T(i)/\alpha G_o(i) - 1|$.

$m = 27$. w_i are, 2, 5, 6, 7, 8, 8.25, 8.5, $\cdots$, 12, 13, $\cdots$, 18 GHz. All frequencies will be multiplied by 2Π and then normalized to (divided by) 20Π GHz.

$G_o(i) = 15.9$ in the passband 8–12 GHz, and unity otherwise.

$w(i)$ are zero out of the passband, 2 at the band-edges 8 and 12 GHz, and unity within the passband.

$N_e = N_f = 2$. Low-pass types for both M_i and M_o assumed, so $k = 0$ in (7)–(8), and $h_{e0} = h_{f0} = 0$. (Band-pass response can be obtained by shunting an inductor to $y_{ii}, i = 1$ or 2. See [9]).

Initial values: $h_{e1} = 1, h_{e2} = -1$, and $h_{f1} = 1, h_{f2} = 1$.

A trial run with $\alpha = 0.326$ resulted in $h_{e1} = -0.724, h_{e2} = 0.992$, and $h_{f1} = 0.148, h_{f2} = 0.382$. The corresponding gain is 7.12 ± 0.48 dB. The GTDRV was repetitively executed using the h_{ej} and h_{fj} just obtained in the last run as initial values accompanied with a gradually increased α. The values of α taken were 0.326, 0.35, 0.4, 0.45, 0.5, and 0.6. When α was finally increased to 0.6, the resultant input reflection functions are

$$e_{11}(s) = \frac{0 - 0.0322s + 0.9219s^2}{1 + 1.3583s + 0.9219s^2},$$
$$f_{11}(s) = \frac{0 + 0.3795s + 0.4827s^2}{1 + 1.0533s + 0.4827s^2}, \quad (11)$$

The transducer power gain in the passband is 9.67 ± 0.56 dB, as shown in Fig. 6. The stability factors evaluated at frequencies, 2, 3, 4, up to 18 GHz are depicted by curve C in Fig. 2. The minimum value of K is 2.07, found at 14 GHz. The corresponding circuit is given in Fig. 3. Increasing α above 0.6 made the ripple larger.

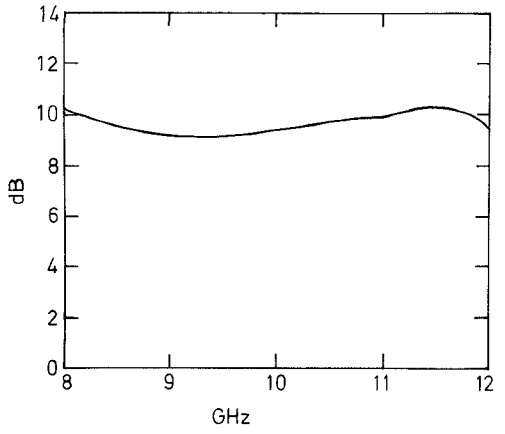

Fig. 6. Transducer power gain of the amplifier in Fig. 3.

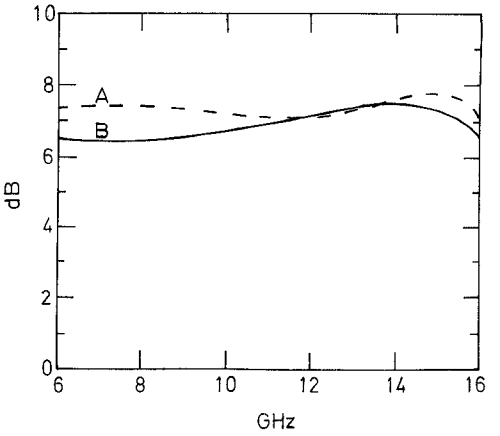

Fig. 7. Transducer power gains of amplifiers in Fig. 4 (curve B) and Fig. 5 (curve A).

The optimization time (input and output time excluded) is within 1.8 second for each execution of GTDRV on PC (80486-33).

Example 2

This example is same as example 1 in [6]. The source and load terminations are 50 ohm. The transistor used is HFET-2001 (Hewlett Packard) with bias $V_{ds} = 4.0$ V and $I_{ds} = 0.5\,Idss$. The passband is 6–16 GHz. It is shown by curve B in Fig. 2 that this transistor is potentially unstable for frequencies below 10 GHz, because its K factor is smaller than 1 in this region.

The input conditions are:

lower and upper limits of both h_{ej} and h_{fj}: -5 and 5, respectively. $errlb = 0.15; m = 11; \omega_i$ are 6, 7, $\cdots$, 15, and 16 GHz. All frequencies will be multiplied by 2Π and then normalized to 20Π GHz. Transistor parameters at 7, 9, 11, 13, and 15 GHz were obtained by interpolating using TOUCHSTONE [13] based on the parameters listed in [6].

$G_o(i) = 10$ from 6–16 GHz.

$w(i) = 1, i \neq 11. w(11) = 2.$

$N_e = 2, N_f = 2$. Low-pass for both M_i and M_o are assumed, so $k = 0$ in (7)–(8), and $h_{e0} = h_{f0} = 0$.

Initial values:

$h_{e1} = 1, h_{e2} = -1$, and $h_{f1} = 1, h_{f2} = -1$.

A trial run with $\alpha = 0.5$ resulted in

$$h_{e1} = -0.001, h_{e2} = 0.176;$$
$$h_{f1} = 0.521, h_{f2} = 0.162. \tag{12}$$

The corresponding gain is 6.81 ± 0.34 dB. Re-ran the GTDRV starting from the h_{ej} and h_{fj} just obtained and setting $\alpha = 0.55$ ended up with

$$e_{11}(s) = \frac{0 - 0.0424s + 0.2023s^2}{1 + 0.6375s + 0.2023s^2},$$
$$f_{11}(s) = \frac{0 + 0.5590s}{1 + 0.5590s} \tag{13}$$

where the second degree coefficients of $f_{11}(s), h_{f2}$ and g_{f2}, are 0.00001 and have been neglected. The circuit realized is given in Fig. 4. The stability factor is shown by curve E in Fig. 2, the minimum value is 7.79, found at 16 GHz. The gain is 6.96 ± 0.51 dB, as detailed by curve B in Fig. 7. For comparison, the amplifier using the same HFET-2001 transistor with $N_e = 2$ and $N_f = 3$ designed by Yarman using Supercompact has a gain of 6.81 ± 0.57 dB [6].

For comparison with the result of example 1 designed by using the more advanced dynamic CAD technique [6], the GTDRV was re-run with $N_e = 2$, and $N_f = 3$ such that the complexities of M_i and M_o are identical with those in [6]. The initial value were those shown in (12) augmented with $h_{f3} = 0.001$. Letting $\alpha = 0.6$ and $errlb = 0.1$ resulted in

$$e_{11}(s) = \frac{0 - 0.1304s + 0.2518s^2}{1 + 0.7216s + 0.2518s^2},$$
$$f_{11}(s) = \frac{0 + 1.1940s + 0.2791s^2 + 0.5870s^3}{1 + 1.7833s + 0.8773s + 0.5870s^3}, \tag{14}$$

The circuit realized is given in Fig. 5. The stability factor is depicted by curve D in Fig. 2; the minimum value is 7.9, found at 16 GHz. The gain is 7.42 ± 0.34 dB, as shown by curve A in Fig. 7. Although the gain obtained here is just slightly higher than that obtained by the dynamic CAD technique (7.35 ± 0.33 dB) [6], the proposed method is simpler in that the M_i and M_o are optimized simultaneously, not generated one-by-one. Besides, the stability requirement has been built in the design process, with a specifiable minimum safety margin. The optimization time is within 2.3 seconds for each execution of GTDRV on PC (80486-33) for this example.

IV. Conclusion

The proposed method allows designing a broadband microwave amplifier with guaranteed stability when employing a potentially unstable transistor. In this method, the simplified real frequency technique [1] is modified such that the objective function decides the amount of deviation from the prescribed transducer power gain of the amplifier, rather than of the matching circuits. This enables simultaneous determination of both the input and output matching circuits. Hence, the design procedure is simplified. The stability is maintained, with a selectable minimum K factor, by incorporating stability constraint functions with the objective function. Exact gradients of the objective and constraint functions are employed in the design program. This obviates the truncation, cancellation, and rounding errors associated with the finite difference approximation [1], [2], [8]. The validity and advantages of the proposed method have been demonstrated by two design examples.

References

[1] B. S. Yarman, "A simplified real frequency technique for broadband matching a complex source to a complex load," *RCA Review*, vol. 43, pp. 529–541, Sept. 1982.

[2] B. S. Yarman and H. J. Carlin, "A simplified real frequency technique applied to broadband multistage microwave amplifiers," *IEEE Trans. Microwave Theory Tech.*, vol. MTT-30, pp. 2216–2222, Dec. 1982.

[3] Compact Software User's Guide, Microwave Harmonica^{R} PC, vol. 1.1. 483, Paterson, NJ.

[4] W. L. Jung and Jingshown Wu, "Stable broadband microwave amplifier design," *IEEE Trans. Microwave Theory Tech*, vol. 38, pp. 1079–1085, Aug. 1990.
[5] H. J. Carlin, "A new approach to gain-bandwidth problems," *IEEE Trans. Circuits Syst.*, vol. CAS-24, pp. 170–175, Apr. 1977.
[6] B. S. Yarman, "A dynamic CAD technique for designing broadband microwave amplifiers," *RCA Review*, vol. 44, pp. 551–565, Dec. 1983.
[7] IMSL User's Manual, MATH/LIBRARY&\trade; , FORTRAN subroutines for mathematical applications, version 1.1, Jan. 1989. IMSL customer relations, Houston.
[8] K. M. Brown and J. E. Dennis, "Derivative free analogues of the Levenberg–Marquardt and Guass algorithms for nonlinear least square approximations," *Numerische Mathematik*, vol. 18, p. 289, 1972.
[9] H. J. Carlin, and J. J. Komiak, "A new method of Broad-band equalization applied to microwave amplifiers," *IEEE Trans. Microwave Theory Tech.*, vol. MTT-27, pp. 93–99, Feb. 1979.
[10] M. S. Ghausi, *Principles and Design of Linear Active Circuits*. New York: McGraw-Hill, 1965.
[11] NEC Corporation, "NE700, low cost Ku-Band GaAs MESFET," 1983, Santa Clara, CA.
[12] W. L. Jung and Jingshown Wu, "Broadband amplifier design with stability consideration," *Int. J Electronics*, vol. 68, no. 2, pp. 209–221, 1990.
[13] EESOF, Touchstone^{R}, User's Manual, EESOF Inc., West Lake Village, CA 91362, Aug. 1986.
[14] G. C. Temes and J. W. LaPatra, *Introduction to Circuit Synthesis and Design* New York: McGraw-Hill, 1977.
[15] T. R. Cuthbert JR, *Optimization Using Personal Computers with Applications to Electrical Networks*. New York: Wiley, 1987.

Extraction of Device Noise Sources from Measured Data Using Circuit Simulator Software

Pertti K. Ikalainen

***Abstract*— A procedure is presented for extracting the properties of device noise sources from experimental data. The extraction procedure can be implemented using commercially available circuit simulators. An example concerning a low-noise pseudomorphic HEMT shows that the two noise sources extracted from experimental data are largely uncorrelated provided that parasitic elements are de-embedded from the measurement and that the sources are extracted in H-parameter format.**

I. Introduction

It is usual to characterize the noise performance of a microwave device with four noise parameters: minimum noise figure $F_{\min}$, optimum source admittance Y_{opt}, and equivalent noise resistance R_n. Together with S-parameters they completely characterize the small-signal performance of any two-port device. However, it is sometimes desirable and physically more meaningful to examine the noise performance in terms of two noise sources associated with the two-port. The four parameters then become the strength of the two sources and the (complex) cross-correlation between them. These two sources can be separated from the two-port in a number of ways, and the theoretical procedures for treating these cases are well established [1], [2].

Given experimental noise parameters (in terms of $F_{\min}, Y_{opt}$, and R_n) and S-parameters, we need an extraction procedure to find the properties of the noise sources. It is also frequently desirable to de-embed the effects of known device parasitics before extracting the noise sources. One such de-embedding and extraction procedure was presented for FETs in [3]. However, that method requires software for conversion between Z and Y correlation matrices. It is the purpose of this paper to report a simple extraction method using commercially available circuit simulation software. This method is general and works for any kind of two port device.

Manuscript received March 30, 1992; revised June 19, 1992.

The author is with Texas Instruments Incorporated, P.O. Box 655936, MS 134, Dallas, TX 75265.

IEEE Log Number 9204469.

II. Extraction of Noise Sources From Measured Data

Consider the noise equivalent representation of Fig. 1(a) [1], [2]. Since knowledge of the strength and cross-correlation of the two noise current sources along with the Y-parameters of the network uniquely determines the four noise parameters, it then follows that, conversely, the noise currents can be uniquely determined from a knowledge of the Y-parameters and the four noise parameters. Equations could be written for the noise sources directly in terms of Y-parameters and $F_{\min}, Y_{opt}$, and R_n. However, it is convenient to first convert the standard noise parameters $F_{\min}, Y_{opt}$, and R_n into a format compatible with the noise equivalent representation of Fig. 1(b) [1], [2]

$$Y_c = \frac{F_{\min} - 1}{2R_n} - Y_{opt} \tag{1}$$

$$G_n = (F_{\min} - 1)\left(G_{opt} - \frac{F_{\min} - 1}{4R_n}\right), \tag{2}$$

where Y_c is the correlation admittance between i_n and e_n of Fig. 1(b)

$$Y_c = \frac{\langle i_n e_n^* \rangle}{\langle e_n e_n^* \rangle}, \tag{3}$$

and G_n is related to the strength of the completely uncorrelated part i_{nu} of i_n of Fig. 1(b)

$$G_n = \frac{\langle |i_{nu}|^2 \rangle}{4kT_0B} = \frac{\langle |i_n - Y_c e_n|^2 \rangle}{4kT_0B}, \tag{4}$$

where k is the Boltzmann constant, T_0 is the standard reference temperature of 290 K, and B is the incremental bandwidth. The brackets $\langle\,\rangle$ indicate time average and * indicates complex conjugation. R_n is related to the strength of e_n of Fig. 1(b) by

$$R_n = \frac{\langle |e_n|^2 \rangle}{4kT_0B}, \tag{5}$$

We now can write equations for i_{n1} and i_{n2} of Fig. 1(a) in terms of R_n, G_n, and Y_c utilizing definitions (3)–(5) and the transformation [2] between i_{n1} and i_{n2} of Fig. 1(a), and i_n and e_n of Fig. 1(b), respectively,

$$\langle |i_{n1}|^2 \rangle = 4kT_0B(G_n + R_n|Y_{11} - Y_c|^2) \tag{6}$$

$$\langle |i_{n2}|^2 \rangle = 4kT_0BR_n|Y_{21}|^2 \tag{7}$$

$$\frac{\langle i_{n1} i_{n2}^* \rangle}{\sqrt{\langle |i_{n1}|^2 \rangle \langle |i_{n2}|^2 \rangle}} = \frac{Y_{21}^*(Y_{11} - Y_c)}{|Y_{21}|\sqrt{\dfrac{G_n}{R_n} + |Y_{11} - Y_c|^2}}. \tag{8}$$

It is interesting to note that the only Y-parameters that enter into (6)–(8) are Y_{11} and Y_{21}. Equations (1), (2), and (6)–(8) can be programmed in a commercial circuit simulator with "output equation" capability. For example, we have used LIBRA and TOUCHSTONE [4] in the examples discussed later in this paper.